—

Casimir cascades in two-dimensional turbulence

John C. Bowman†

Department of Mathematical and Statistical Sciences, University of Alberta, Edmonton,
Alberta T6G 2G1, Canada

In addition to conserving energy and enstrophy, the nonlinear terms of the two-dimensional incompressible Navier–Stokes equation are well known to conserve the global integral of any continuously differentiable function of the scalar vorticity field. However, the phenomenological role of these additional inviscid invariants, including the issue as to whether they cascade to large or small scales, is an open question. In this work, well-resolved implicitly dealiased pseudospectral simulations suggest that the fourth power of the vorticity cascades to small scales.

Key words: computational methods, turbulence simulation, turbulence theory

1. Two-dimensional turbulence

The Kraichnan–Leith–Batchelor theory of two-dimensional incompressible turbulence relies on the fact that the nonlinear terms of the two-dimensional Navier–Stokes equation conserve both energy and enstrophy (Kraichnan 1967, 1971; Leith 1968; Batchelor 1969). Consequently, in an infinite domain and in the limit of infinite Reynolds number, the net energy and enstrophy transfers outside of a localized forcing region must be independent of wavenumber. The predicted dual cascade of energy to larger scales and enstrophy to smaller scales is readily observed in numerical simulations of two-dimensional turbulence in a bounded periodic domain.

It is well known that the nonlinearity of the two-dimensional Navier–Stokes equation in addition conserves the global integral of any arbitrary piecewise continuous function of the scalar vorticity field. While it is known that these so-called Casimir invariants arise from an underlying rearrangement symmetry (corresponding to the conservation of vorticity measure), their precise physical role remains an open question. For example, it is not known whether they could play a fundamental role in the turbulent cascade, just like energy and enstrophy. In particular, do Casimir invariants exhibit cascades? In the literature, Polyakov's minimal conformal field theory model (Polyakov 1993) predicts that the higher-order Casimir invariants cascade to large scales, while Falkovich & Hanany (1993) and Eyink (1996) suggest that they might instead cascade to small scales.

Numerical investigations of these questions are hampered by the fact that pseudospectral simulations, which necessarily truncate the wavenumber domain, do not conserve these higher-order Casimir invariants, unlike the so-called *rugged* quadratic (energy and enstrophy) invariants, which do survive wavenumber truncation. In this

† Email address for correspondence: bowman@math.ualberta.ca

work, we establish that it is nevertheless possible to demonstrate with sufficiently well-resolved simulations that the fourth power of the vorticity is transferred to smaller scales.

2. Casimir invariants

We begin with the two-dimensional incompressible Navier–Stokes equation for the *vorticity* $\omega \doteq \hat{z} \cdot \nabla \times u$ ($\doteq$ is used to emphasize a definition),

$$\frac{\partial \omega}{\partial t} + u \cdot \nabla \omega = \nu \nabla^2 \omega + f, \tag{2.1}$$

where the constant ν is the kinematic viscosity and f represents a white-noise stochastic stirring. In the inviscid unforced limit $\nu = f = 0$, both the *energy* $E \doteq \frac{1}{2} \int u^2 \, dx$ and *enstrophy* $Z \doteq \frac{1}{2} \int \omega^2 \, dx$ are conserved.

However, as is well known, inviscid unforced two-dimensional turbulence has uncountably many other *Casimir* invariants. For example, any (piecewise) continuously differentiable function F of the (scalar) vorticity is conserved by the nonlinearity:

$$\frac{d}{dt} \int F(\omega) \, dx = \int F'(\omega) \frac{\partial \omega}{\partial t} \, dx = -\int F'(\omega) u \cdot \nabla \omega \, dx$$

$$= -\int u \cdot \nabla F(\omega) \, dx = \int F(\omega) \nabla \cdot u \, dx = 0.$$

Although it is not known whether these additional invariants play a fundamental role in the turbulent dynamics, it is certain that only the quadratic invariants, which are a consequence of detailed triadic balance, survive high-wavenumber truncation. To see this, one can express (2.1) in Fourier space:

$$\frac{\partial \omega_k}{\partial t} + \nu_k \omega_k = \sum_{p,q} \frac{\epsilon_{kpq}}{q^2} \omega_p^* \omega_q^* + f_k, \tag{2.2}$$

where $\nu_k \doteq \nu k^2$ and $\epsilon_{kpq} \doteq (\hat{z} \cdot p \times q) \, \delta(k + p + q)$ is seen to be antisymmetric under interchange of any two indices. When $\nu_k = f_k = 0$, the enstrophy is readily seen to be conserved:

$$\frac{d}{dt} \sum_k |\omega_k|^2 = \sum_{k,p,q} \frac{\epsilon_{kpq}}{q^2} \omega_k^* \omega_p^* \omega_q^* = 0, \tag{2.3}$$

noting the antisymmetry of the summand in $k \leftrightarrow q$. In the absence of high-wavenumber truncation, the invariance of

$$Z_3 \doteq \frac{1}{(2\pi)^4} \int \omega^3 \, dx = \sum_{k,r} \omega_k \omega_r \omega_{-k-r} = \sum_{k,r,s} \omega_k \omega_r \omega_s \delta_{k+r+s,0} \tag{2.4}$$

appears in Fourier space as the identity

$$0 = \frac{d}{dt} Z_3 = 3 \sum_{k,r,s} \frac{\partial \omega_k}{\partial t} \omega_r \omega_s \delta_{k+r+s,0} = \sum_{k,r,s} \sum_{p,q} \frac{\epsilon_{kpq}}{q^2} \omega_p^* \omega_q^* \omega_r \omega_s \delta_{k+r+s,0}. \tag{2.5}$$

However, the absence of an explicit ω_k in the final summand means that setting $\omega_\ell = 0$ for $\ell > K$ will break the symmetry in the summation limits. Nevertheless, since the missing terms involve modes higher than the truncation wavenumber K, one might expect that a very well-resolved simulation would lead to almost exact invariance of Z_3. We will see that this is indeed the case.

3. Cumulative enstrophy transfer

In terms of the nonlinearity $S_k \doteq \sum_{p,q}(\epsilon_{kpq}/q^2)\omega_p^*\omega_q^*$, the enstrophy spectrum $Z(k)$ is seen to satisfy a balance equation of the form

$$\frac{\partial}{\partial t}Z(k) + 2\nu_k Z(k) = 2T(k) + G(k), \tag{3.1}$$

where $T(k)$ and $G(k)$ represent angular sums of $\mathrm{Re}\langle S_k \omega_k^* \rangle$ and $\mathrm{Re}\langle f_k \omega_k^* \rangle$, respectively. Following Kraichnan (1959), it is convenient to define the *nonlinear enstrophy transfer* $\Pi(k)$, which measures the cumulative nonlinear transfer of enstrophy into $[k, \infty)$:

$$\Pi(k) = 2\int_k^\infty T(p)\,\mathrm{d}p. \tag{3.2}$$

On integrating from k to ∞, we find

$$\frac{\mathrm{d}}{\mathrm{d}t}\int_k^\infty Z(p)\,\mathrm{d}p = \Pi(k) - \eta(k), \tag{3.3}$$

where $\eta(k) \doteq 2\int_k^\infty \nu_p Z(p)\,\mathrm{d}p - \int_k^\infty G(p)\,\mathrm{d}p$ is the total enstrophy transfer, via dissipation and forcing, out of wavenumbers higher than k. A positive (negative) value for $\Pi(k)$ represents a flow of enstrophy to wavenumbers higher (lower) than k. When $\nu_k = f_k = 0$, enstrophy conservation implies that

$$0 = \frac{\mathrm{d}}{\mathrm{d}t}\int_0^\infty Z(p)\,\mathrm{d}p = 2\int_0^\infty T(p)\,\mathrm{d}p, \tag{3.4}$$

so that

$$\Pi(k) = 2\int_k^\infty T(p)\,\mathrm{d}p = -2\int_0^k T(p)\,\mathrm{d}p. \tag{3.5}$$

We note that $\Pi(0) = \Pi(\infty) = 0$. Moreover, in a steady state, $\Pi(k) = \eta(k)$; this provides an excellent numerical diagnostic for validating a steady state.

The cumulative nonlinear enstrophy transfer Π_3 for the globally integrated invariant $Z_3 = \int \omega^3\,\mathrm{d}x$ can be defined similarly and measured numerically. However, we found no systematic cascade of Z_3; this invariant appears to slosh back and forth between the large and small scales. In hindsight, this should be expected since ω^3 is not a sign-definite quantity.

Of much more interest is the determination, using a pseudospectral code, of the cascade direction of a sign-definite quantity like the fourth-order Casimir invariant $\int \omega^4\,\mathrm{d}x$. If we Fourier-decompose $Z_4 \doteq N^3\sum_j \omega^4(x_j)$ in terms of N spatial collocation points x_j, we find

$$Z_4 = \sum_{k,p,q} \omega_k \omega_p \omega_q \omega_{-k-p-q}. \tag{3.6}$$

It is worthwhile here to mention some details regarding the numerical implementation of the stochastic forcing. We advance the vorticity equation $\mathrm{d}\omega_k/\mathrm{d}t = [S_k - \nu_k\omega_k] + f_k$, where S_k represents the nonlinear source term, using operator splitting: while a fifth-order adaptive Cash–Karp Runge–Kutta integrator is used for the deterministic part $S_k - \nu_k\omega_k$, the stochastic stirring force f_k is treated separately as an additive random source, to avoid severe time-step restrictions. A single time step of

the integration method may be formally represented by the discrete mapping

$$\widetilde{\omega}_k = \omega_k(t_n) + \int_{t_n}^{t_{n+1}} S_k(\tau)\,\mathrm{d}\tau, \tag{3.7a}$$

$$\omega_k(t_{n+1}) = \widetilde{\omega}_k + \sqrt{2(t_{n+1} - t_n)} f_k, \tag{3.7b}$$

where it is implicitly understood that S_k also depends on all of the modes ω_k. Between times t_n and t_{n+1}, this prescription yields a mean enstrophy injection

$$\begin{aligned}
\tfrac{1}{2}[\langle|\omega_k(t_{n+1})|^2\rangle - \langle|\widetilde{\omega}_k|^2\rangle] &= \tfrac{1}{2}\langle|\widetilde{\omega}_k + \sqrt{2(t_{n+1}-t_n)}f_k|^2\rangle - \tfrac{1}{2}\langle|\widetilde{\omega}_k|^2\rangle \\
&= \sqrt{2(t_{n+1}-t_n)}\,\mathrm{Re}\,\widetilde{\omega}_k\,\langle f_k^*\rangle + (t_{n+1}-t_n)\langle|f_k|^2\rangle \\
&= (t_{n+1}-t_n)\langle|f_k|^2\rangle, \tag{3.8}
\end{aligned}$$

using the fact that $\langle f_k\rangle = 0$. The mean rate of enstrophy injection is thus $\eta = \sum_k \langle|f_k|^2\rangle$, in accord with a theorem of Novikov (1964). The contribution to $G(k)$ arising from the stirring force f_k between times t_n and t_{n+1} is consequently the ensemble average of

$$\tfrac{1}{2}|\omega_k(t_{n+1})|^2 - \tfrac{1}{2}|\widetilde{\omega}_k|^2 = \tfrac{1}{2}|\widetilde{\omega}_k + \sqrt{2(t_{n+1}-t_n)}f_k|^2 - \tfrac{1}{2}|\widetilde{\omega}_k|^2. \tag{3.9}$$

On differentiating (3.6) with respect to time, one can express the evolution of Z_4 in terms of the nonlinear source term S_k as

$$\frac{\mathrm{d}}{\mathrm{d}t}Z_4 = \sum_k\left[S_k\sum_{p,q}\omega_p\omega_q\omega_{-k-p-q} + 3\omega_k\sum_{p,q}S_p\omega_q\omega_{-k-p-q}\right] = \sum_k T_4(k), \tag{3.10}$$

where

$$T_4(k) \doteq N^2\sum_{|k|=k}\left[S_k\sum_j\omega^3(x_j)\mathrm{e}^{2\pi\mathrm{i}j\cdot k/N} + 3\omega_k\sum_j S(x_j)\omega^2(x_j)\mathrm{e}^{2\pi\mathrm{i}j\cdot k/N}\right]. \tag{3.11}$$

Here $S(x_j)$ is the inverse Fourier transform of S_k.

The contribution to the transfer of Z_4 arising from the stirring force f_k between times t_n and t_{n+1} can be computed as

$$G_4(k) \doteq N^2\sum_{|k|=k}\left[\omega_k\sum_j\omega^3(x_j)\mathrm{e}^{2\pi\mathrm{i}j\cdot k/N} - \widetilde{\omega}_k\sum_j\widetilde{\omega}^3(x_j)\mathrm{e}^{2\pi\mathrm{i}j\cdot k/N}\right], \tag{3.12}$$

where ω_k and its inverse Fourier transform ω are evaluated at t_{n+1}. The contribution $D_4(k)$ to the transfer of Z_4 arising from dissipation is given by the same form as $T_4(k)$ with S_k replaced by $-\nu_k\omega_k$.

We then define

$$\Pi_4(k) \doteq \int_k^\infty T_4(p)\,\mathrm{d}p = -\int_0^k T_4(p)\,\mathrm{d}p \tag{3.13}$$

to measure the cumulative nonlinear transfer of Z_4 into $[k,\infty)$ and

$$\eta_4(k) \doteq \int_k^\infty D_4(p)\,\mathrm{d}p - \int_k^\infty G_4(p)\,\mathrm{d}p \tag{3.14}$$

to represent the contribution to the transfer of Z_4 arising from dissipation and forcing out of $[k, \infty)$. We note that $\Pi_4(0) = \Pi_4(\infty) = 0$. As with the enstrophy transfer balance, it is easily seen that $\Pi_4(k) = \eta_4(k)$ in a steady state.

4. Implementation

An important point to emphasize in computing $T_4(k)$ and $G_4(k)$ is that (3.10) requires the computation of a ternary convolution $\sum_{p,q} \omega_p \omega_q \omega_{-k-p-q}$ in terms of the Fourier transform of the cubic quantity ω^3. Correctly dealiasing therefore requires a $1/2$ zero padding rule (instead of the usual $2/3$ rule for a binary convolution), so that, in two dimensions, only 25% of the computation buffer contains physical data. To avoid the extreme waste of memory and computation time associated with padding the other 75% of the data buffer with zeros and then reading and multiplying these zero values by primitive roots of unity, we have developed optimized implicitly dealiased algorithms to compute the required ternary convolutions without padding (Bowman & Roberts 2011). These algorithms, which we have made publicly available in our open-source library FFTW++ (Bowman & Roberts 2010), are most efficient when the dimension of the physical data in each direction is one less than a power of 2. For example, dealiased ternary convolutions on a 2047×2047 Fourier data array would require a 4096×4096 data buffer with conventional explicit zero padding. In both cases, the maximum retained physical wavenumber in each direction is 1023. Implicit dealiasing of a two-dimensional ternary convolution allows the identical calculation to be performed using roughly half of the memory that would be required by the zero-padding technique.

To avoid having to develop specialized routines for computing a ternary convolution, it might at first seem possible to compute a ternary convolution as a double convolution. In one dimension one can certainly write $e_k = f_p g_q h_{k-p-q} = f_p c_{k-p}$, where, letting $r \doteq k - p$, we first compute the intermediate convolution $c_r \doteq g_q h_{r-q}$. Here k, p and q all run from $-m+1$ to $m-1$, so that we need to know c_r for r values running from $-2m+2$ to $2m-2$. A conventional dealiased convolution routine would have to be extended to compute all of these outputs. This would require that $3m - 3 - N < -m+1$. For $2m-1$ data values, one needs $N > 4m-4$, which essentially corresponds to a $1/2$ padding rule. Given that the resulting padding ratios are identical, computing a ternary convolution directly is more efficient than the double convolution approach (which would already require a modified routine to compute c_r for additional r values) as it avoids extra computation, storage, and retrieval of intermediate quantities. We emphasize that a linear ternary convolution cannot be computed via two dealiased binary convolutions truncated to the size of the data vector. For example, the $(m-1)$th component of the ternary convolution of vectors f, g and h indexed from $-m+1$ to $m-1$ will include the term $f_{m-1} g_{m-1} h_{-m+1}$. However, computing $(f*g)*h$ using two conventional binary convolutions excludes this term, as $f_{m-1} g_{m-1}$ does not contribute to the $2m-1$ retained components of $f*g$ (Roberts & Bowman 2011).

5. Numerical results

To investigate the cascade direction of Z_4, we consider a doubly periodic dealiased pseudospectral simulation with 1023×1023 physical Fourier modes driven in the wavenumber interval $[1.5, 2.5]$ by a white-noise stochastic stirring force f_k with prescribed enstrophy injection rate $\eta = 1$. We replace the molecular dissipation term by $\nu_k = \nu_H H(k_L - k) + \nu_L k^2 H(k - k_H)$, where H is the Heaviside step function. The cutoff wavenumbers $k_L = 3.0001$ and $k_H = 260$, with $\nu_L = 0.2$ and $\nu_H = 4 \times 10^{-5}$, mimic
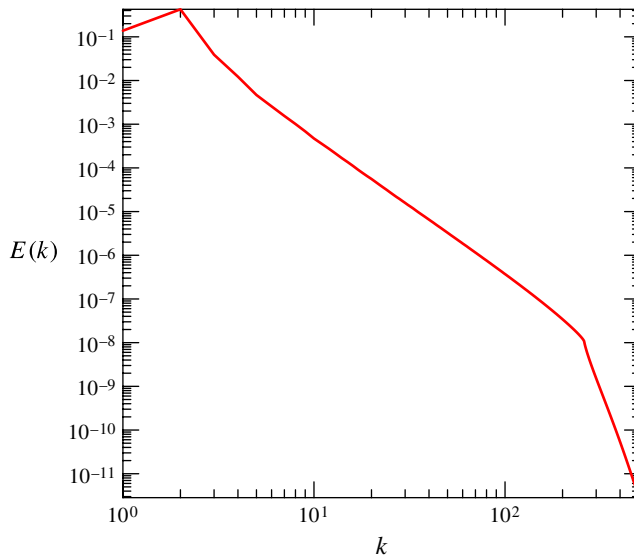
FIGURE 1. (Colour online) Steady-state energy spectrum of 1023×1023 dealiased modes forced in the band [1.5, 2.5].
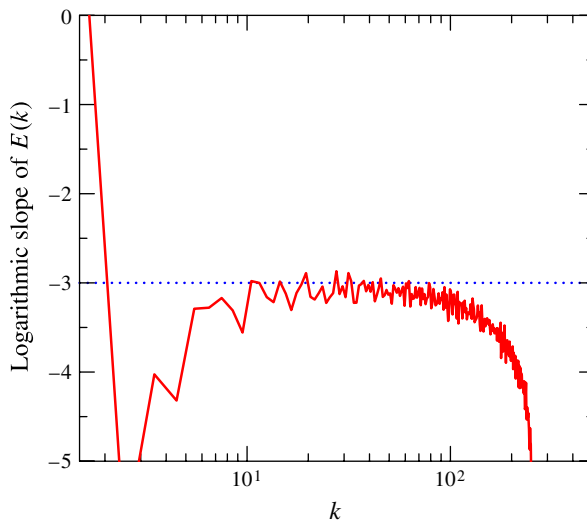

FIGURE 2. (Colour online) Logarithmic slope of the energy spectrum in figure 1.

the idealization of a pristine inertial range in an unbounded spatial domain, the limit addressed by the Kraichnan–Leith–Batchelor theory.

The resulting mean energy spectrum, shown in figure 1, and corresponding slope, shown in figure 2, indicate that the sharp high-wavenumber viscosity cutoff introduces very little of the usual kind of bottleneck effect observed with lower-order hyperviscous damping and instead yields the logarithmically corrected k^{-3} spectrum shown in figure 3 (Kraichnan 1971; Bowman 1996). In figure 4, we observe that the time-averaged nonlinear enstrophy transfer $\Pi(k)$ is positive and constant in the
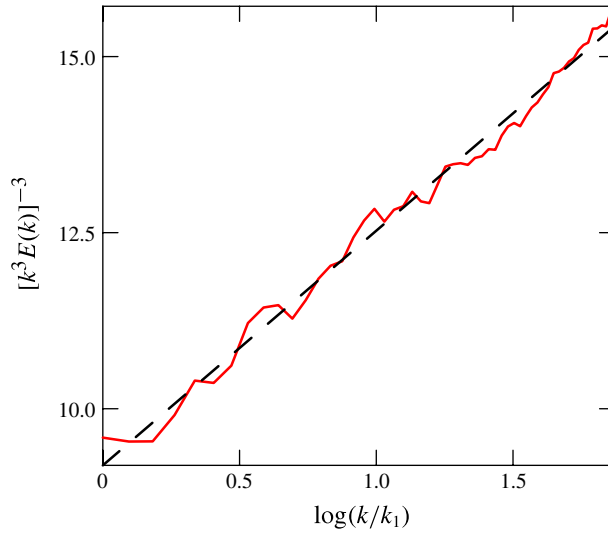
FIGURE 3. (Colour online) Verification of the logarithmic correction $[\log(k/k_1)]^{-1/3}$ to the inertial range k^{-3} energy spectrum in figure 1 or $k \in [k_1, k_2] = [10, 65]$. The dashed line represents a least-squares fit.
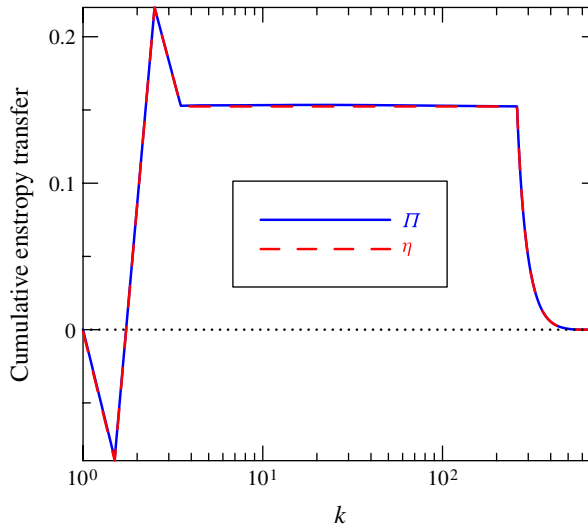

FIGURE 4. (Colour online) Nonlinear transfer of Z downscale from the forcing band [1.5, 2.5].

enstrophy inertial range; this indicates that enstrophy is transferred to small scales. We conclude from the coincidence of the graphs of the nonlinear transfer $\Pi(k)$ and linear transfer $\eta(k)$ that injection, nonlinear transfer, and dissipation are in balance.

In figure 5, we see that the time-averaged nonlinear transfer Π_4 of Z_4 also exhibits the clear signature of a downscale transfer (positive Π_4 in the enstrophy inertial range). To check that sufficient numerical resolution has been used to resolve the contribution of the nonlinear terms to the evolution of Z_4, we observe that $\Pi_4(0) = \Pi_4(\infty) = 0$.
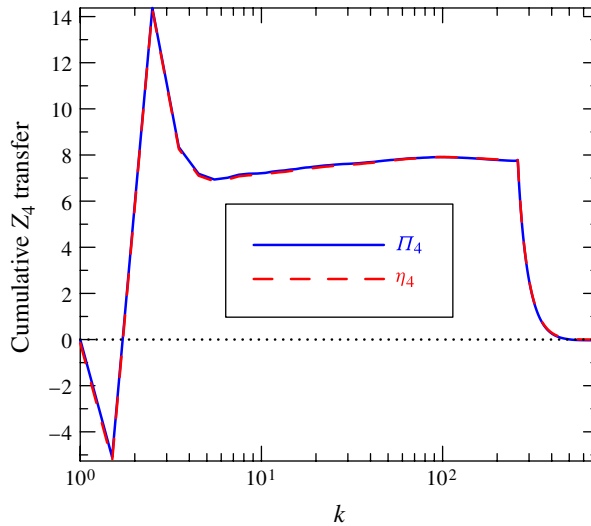
FIGURE 5. (Colour online) Nonlinear transfer of Z_4 downscale from the forcing band [1.5, 2.5].

As an additional diagnostic to ensure that a steady state has been reached, we note that $\Pi_4(k) = \eta_4(k)$. In contrast to figure 4, we observe that the graph of $\Pi_4(k)$ is not completely flat within the inertial range; this is due to the small but non-negligible inertial-range pumping of Z_4 by the large-scale forcing. That is, while the angular sum $G(k)$ of $\text{Re}\langle f_{\boldsymbol{k}}\omega_{\boldsymbol{k}}^*\rangle$ has contributions only when $f_{\boldsymbol{k}}$ is non-zero, $G_4(k)$ receives contributions from the forcing at scales quite different from k, as we see from the first term in (3.12) and as pointed out previously by Falkovich & Lebedev (1994). Therefore, while the enstrophy injected by a localized forcing is local, the injection of Z_4 is not.

In the simulation corresponding to figures 1–5, the forcing scale was deliberately chosen to be close to the domain size, devoting virtually all of the computational resources to the study of the direct cascade. However, this choice inhibited the formation of an inverse energy cascade, characterized by the merger of increasingly large vortices. In view of the fact that Vallgren & Lindborg (2011) report that the intermittency levels in the enstrophy cascade depend greatly on the forcing scale and the presence of an energy cascade, it seems prudent to check whether Z_4 still exhibits a downscale transfer when the turbulence is forced at a significantly higher wavenumber. The steady-state energy spectrum in figure 6 was obtained for a simulation of 2047×2047 physical Fourier modes forced in the band [19.5, 20.5], using the parameters $k_L = 21.0001$ and $k_H = 500$, with $\nu_L = 0.02$ and $\nu_H = 0.0002$. The slopes of the short energy and enstrophy ranges that result are depicted in figure 7, with the logarithmic correction for the enstrophy range illustrated in figure 8. Along with the expected downscale transfer of Z shown in figure 9, we see in figure 10 once again that Z_4 is transferred to scales smaller than the forcing wavenumber.

6. Concluding remarks

Even though higher-order Casimir invariants do not survive wavenumber truncation, it appears possible with sufficiently well-resolved simulations to check whether they
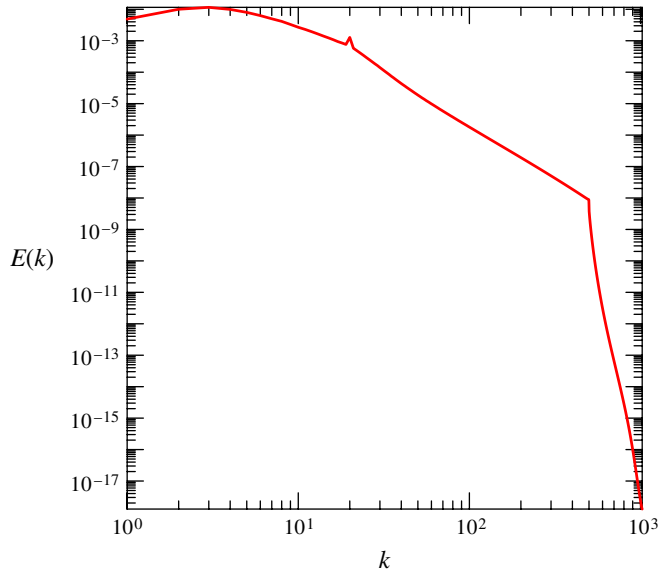
FIGURE 6. (Colour online) Steady-state energy spectrum of 2047×2047 dealiased modes forced in the band [19.5, 20.5].
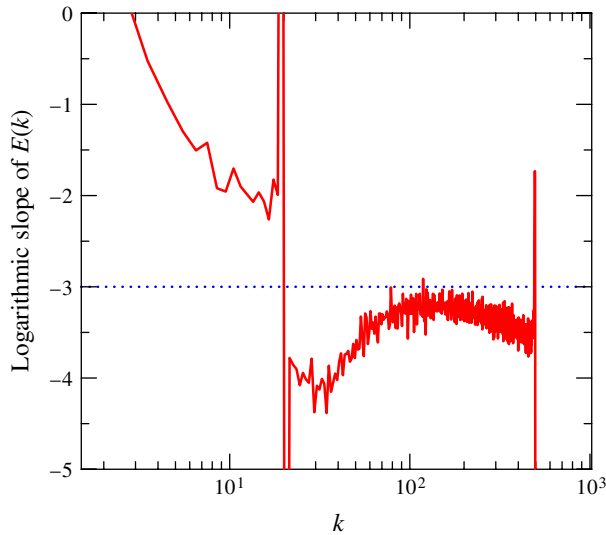

FIGURE 7. (Colour online) Logarithmic slope of the energy spectrum in figure 6.

cascade to large or small scales. In this work, we have computed the transfer of the globally integrated ω^4 inviscid invariant and provided strong numerical evidence supporting the conjectures of Falkovich and Eyink that, in the enstrophy inertial range, there is a direct transfer of (positive-definite) high-order invariants to small scales. While determining the transfer direction of the fourth power of the vorticity would normally require that the domain be doubled in each direction, so that only one-quarter of the simulated Fourier modes are physical, we used the efficient implicitly
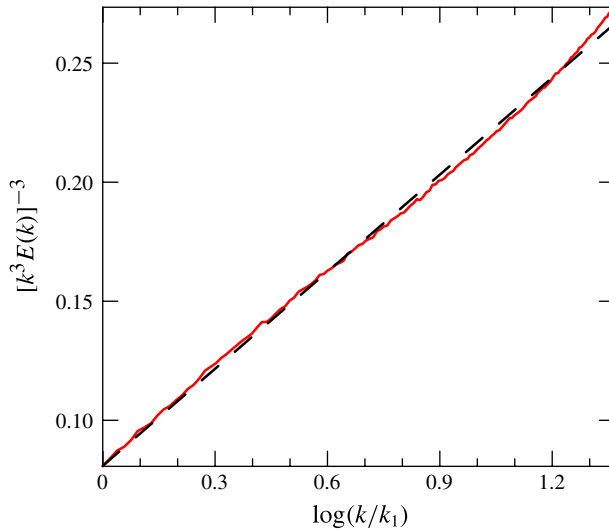
FIGURE 8. (Colour online) Verification of the logarithmic correction $[\log(k/k_1)]^{-1/3}$ to the inertial range k^{-3} energy spectrum in figure 6 for $k \in [k_1, k_2] = [51, 200]$. The dashed line represents a least-squares fit.
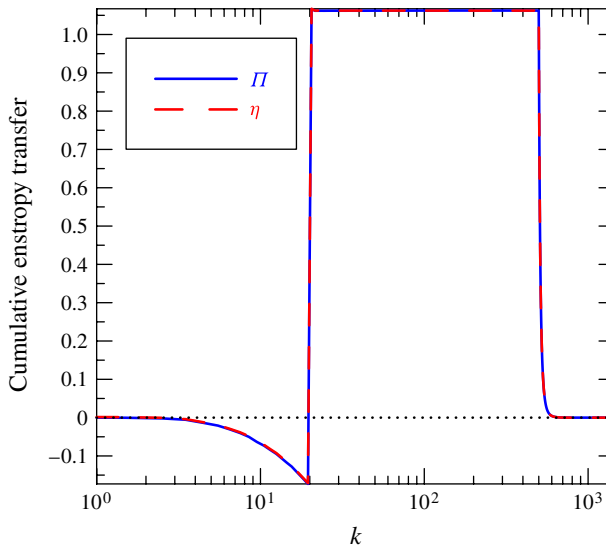

FIGURE 9. (Colour online) Nonlinear transfer of Z downscale from the forcing band [19.5, 21.5].

dealiased ternary convolutions developed in the open-source library FFTW++ to avoid the waste of memory and computation time inherent in explicit zero padding (Bowman & Roberts 2011; Roberts & Bowman 2011, 2012).

As is evident in (2.4) and (3.10), the conservation of high-order Casimir invariants is intricately connected with the symmetries of wave beating. The spectral decomposition of $\mathrm{d}Z_4/\mathrm{d}t$ in (3.10) into sums over wavenumber shells of the quantity $T_4(k)$ elucidates
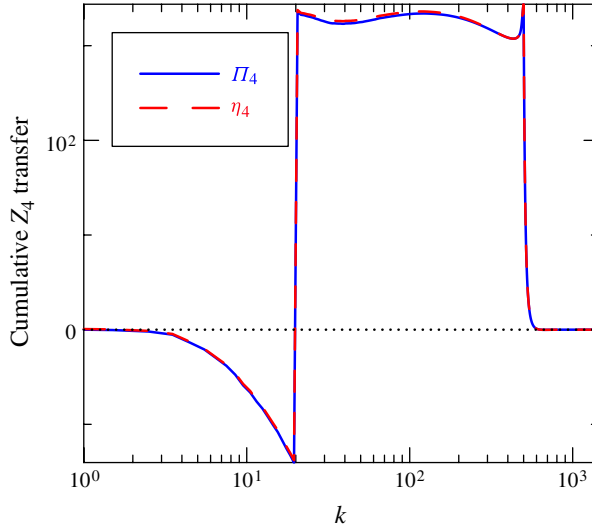
FIGURE 10. (Colour online) Nonlinear transfer of Z_4 downscale from the forcing
band [19.5, 21.5].

this underlying mechanism. Nevertheless, the spectral decomposition of higher-order
moments like $\mathrm{d}Z_4/\mathrm{d}t$ is not unique. For example, the summations in (3.10) may be
readily rearranged to obtain

$$\frac{\mathrm{d}}{\mathrm{d}t}Z_4 = 4 \sum_{k,p,q} S_k \omega_p \omega_q \omega_{-k-p-q} = \sum_k T_4'(k), \tag{6.1}$$

where

$$T_4'(k) = \sum_{|k|=k,p,q} S_k \omega_p \omega_q \omega_{-k-p-q}. \tag{6.2}$$

Alternatively, on denoting $[\omega^2]_k \doteq N^{-1}\sum_p \omega_p \omega_{k-p}$, one could use the factorization
$Z_4 = N^3 \sum_j (\omega^2(x_j))^2$ to express

$$\frac{\mathrm{d}}{\mathrm{d}t}Z_4 = N^2 \frac{\mathrm{d}}{\mathrm{d}t} \sum_k [\omega^2]_k [\omega^2]_{-k} = 2N^2 \,\mathrm{Re}\sum_k \frac{\mathrm{d}[\omega^2]_k}{\mathrm{d}t}[\omega^2]_{-k}, \tag{6.3}$$

so that

$$\frac{\mathrm{d}}{\mathrm{d}t}Z_4 = 4\,\mathrm{Re}\sum_k \left[\sum_p S_p \omega_{k-p}\sum_q \omega_q \omega_{k-q}\right] = \sum_k T_4''(k), \tag{6.4}$$

where

$$T_4''(k) = 4\,\mathrm{Re}\sum_{|k|=k}\sum_p S_p \omega_{k-p}\sum_q \omega_q \omega_{k-q}. \tag{6.5}$$

Under wavenumber truncation, we found by numerical simulation that neither of
the alternative definitions $T_4'(k)$ or $T_4''(k)$ lead to a quasi-flat cumulative fourth-order
transfer in the inertial range like that observed in figures 5 and 10. This is not so

surprising when one considers that wave beating appears asymmetrically in (6.2) (the receiving mode is always mode k) and that the ternary convolution, which expresses three-mode beating, is completely obscured in (6.5). In fact, the scrambling of the various contributions to three-mode beating in (6.5) makes it much more susceptible to high-wavenumber truncation than (3.11) or (6.2). In contrast, the definition of $T_4(k)$ given in (3.11) appears to be the natural extension of $T(k)$ to fourth order.

In closing, we would like to point out an important philosophical distinction between nonlinear enstrophy *transfer* and *flux*. The mean rate of enstrophy transfer to $[k, \infty)$ is given by (3.5). In a steady state, $\Pi(k)$ will thus trivially be constant throughout an inertial range. In contrast, the enstrophy flux through a wavenumber k, as considered by Kolmogorov, is the amount of enstrophy transferred to small scales via triad interactions mediated by mode k. Specifically, on expressing the nonlinear interaction coefficient for the vorticity ω_k as $M_{k,p} = \hat{z} \cdot p \times k / p^2$, where $\hat{z}$ is the unit normal to the plane of motion, the *enstrophy flux* (or exchange) mediated via wavenumber k would need to be computed as a restricted convolution:

$$F_k = \mathrm{Re} \sum_{\substack{|k|=k \\ |p|<k \\ |k-p|<k}} M_{k,p} \omega_p \omega_{k-p} \omega_k^* - \mathrm{Re} \sum_{\substack{|k|=k \\ |p|<k \\ |k-p|>k}} M_{p,k-p} \omega_p \omega_{k-p} \omega_k^*. \tag{6.6}$$

The dependence of restrictions like $|p| < k$ on k makes this calculation difficult to implement efficiently. Kolmogorov's ansatz of self-similar flux suggests that the time average of F_k should be independent of wavenumber. Note that F_k is *not* the same as the total transfer into $[k, \infty)$ unless the transfer is strictly local in wavenumber space (which is not the case for two-dimensional enstrophy transfer). The independence of the flux on k is highly non-trivial and depends on details of the triadic interactions that Kolmogorov conjectured leads to self-similarity in the inertial range. In this work, we have only established that there is a downscale (probably non-local) transfer of Z_4, without actually measuring the flux, as would be needed to establish the existence of a true (self-similar) cascade. Such a cascade, if it exists, would of course be somewhat contaminated by the inertial-range pumping of Z_4 by the localized forcing.

The results of this study raise the question of whether the Kraichnan–Leith–Batchelor theory of unbounded two-dimensional turbulence, based solely on uniform fluxes of energy to large scales and enstrophy to small scales, needs to be re-examined to account for a direct cascade of Casimir invariants to smaller scales. In future work on decaying turbulence, we also plan to measure the decay rate of Casimir invariants like Z_4 and compare these findings to numerical observations and predictions based on conformal field theory by Cateau, Matsuo & Umeki (1993). We would also like to develop analytic estimates for the degree of non-conservation of Casimir invariants due to spectral truncation.

REFERENCES

BATCHELOR, G. K. 1969 Computation of the energy spectrum in homogeneous two-dimensional turbulence. *Phys. Fluids* **12** (II), 233–239.

BOWMAN, J. C. 1996 On inertial-range scaling laws. *J. Fluid Mech.* **306**, 167–181.

BOWMAN, J. C. & ROBERTS, M. 2010 FFTW++: a fast Fourier transform C^{++} header class for the FFTW3 library. http://fftwpp.sourceforge.net.

BOWMAN, J. C. & ROBERTS, M. 2011 Efficient dealiased convolutions without padding. *SIAM J. Sci. Comput.* **33** (1), 386–406.

CATEAU, H., MATSUO, Y. & UMEKI, M. 1993 Predictions on two-dimensional turbulence by conformal field theory. arXiv: hep-th/9310056.

EYINK, G. L. 1996 Exact results on stationary turbulence in 2D: consequences of vorticity. *Physica D* **91**, 97–142.

FALKOVICH, G. & HANANY, A. 1993 Is 2D turbulence a conformal turbulence? *Phys. Rev. Lett.* **71**, 3454–3457.

FALKOVICH, G. & LEBEDEV, V. 1994 Universal direct cascade in two-dimensional turbulence. *Phys. Rev. E* **50** (5), 3883–3899.

KRAICHNAN, R. H. 1959 The structure of isotropic turbulence at very high Reynolds numbers. *J. Fluid Mech.* **5**, 497–543.

KRAICHNAN, R. H. 1967 Inertial ranges in two-dimensional turbulence. *Phys. Fluids* **10** (7), 1417–1423.

KRAICHNAN, R. H. 1971 Inertial-range transfer in two- and three-dimensional turbulence. *J. Fluid Mech.* **47**, 525–535.

LEITH, C. E. 1968 Diffusion approximation for two-dimensional turbulence. *Phys. Fluids* **11**, 671–673.

NOVIKOV, E. A. 1964 Functionals and the random-force method in turbulence theory. *J. Exp. Theor. Phys. (USSR)* **47**, 1919–1926.

POLYAKOV, A. M. 1993 The theory of turbulence in two dimensions. *Nucl. Phys.* B **396**, 367–385.

ROBERTS, M. & BOWMAN, J. C. 2011 Dealiased convolutions for pseudospectral simulations. *J. Phys.: Conf. Ser.* **318** (7), 072037.

ROBERTS, M. & BOWMAN, J. C. 2012 Multithreaded implicitly dealiased pseudospectral convolutions. In *Proceedings of the 20th Annual Conference of the CFD Society of Canada* (ed. R. Martinuzzi & C. Lange), Canmore, Alberta.

VALLGREN, A. & LINDBORG, E. 2011 The enstrophy cascade in forced two-dimensional turbulence. *J. Fluid Mech.* **671**, 168–183.